## **Main Manuscript for:**

# Redox conditions correlated with vibronic coupling modulate quantum beats in photosynthetic pigmentprotein complexes

Jacob S. Higgins<sup>a,b,c,#</sup>, Marco A. Allodi<sup>a,b,c,#</sup>, Lawson T. Lloyd<sup>a,b,c</sup>, John P. Otto<sup>a,b,c</sup>, Sara H. Sohail<sup>a,b,c,1</sup>, Rafael G. Saer<sup>d,f</sup>, Ryan E. Wood<sup>a,b,c</sup>, Sara C. Massey<sup>a,b,c,2</sup>, Po-Chieh Ting<sup>a,b,c</sup>, Robert E. Blankenship<sup>d,e,f</sup>, and Gregory S. Engel<sup>a,b,c,3</sup>

<sup>a</sup>Department of Chemistry, The University of Chicago, Chicago, IL, 60637; <sup>b</sup>The Institute for Biophysical Dynamics, The University of Chicago, Chicago, IL, 60637; <sup>c</sup>The James Franck Institute, The University of Chicago, Chicago, IL, 60637; <sup>d</sup>The Photosynthetic Antenna Research Center, Washington University in St. Louis, St. Louis, MO, 63130; <sup>c</sup>Department of Chemistry, Washington University in St. Louis, St. Louis, MO, 63130; <sup>f</sup>Department of Biology, Washington University in St. Louis, St. Louis, MO, 63130

#### **Keywords**

2D electronic spectroscopy, photosynthesis, vibronic coupling, quantum coherences, Fenna-Matthews-Olson complex

#### Classification

Physical Sciences: Chemistry

#### **Author Contributions**

J.S.H., M.A.A, L.T.L, J.P.O., S.H.S., R.E.W., S.C.M. and P-C.T. performed the experiments. J.S.H., M.A.A, and L.T.L. analyzed the data. R.G.S. and R.E.B. isolated the samples. All authors wrote and edited the manuscript. R.E.B. and G.S.E. designed and oversaw the experiments.

#### This file includes:

Main Text Figures 1 to 4

<sup>&</sup>lt;sup>1</sup> Present address: Laboratory of Chemical Physics, National Institute of Diabetes, and Digestive, and Kidney Diseases, National Institutes of Health, Bethesda, Maryland 20892, United States

<sup>&</sup>lt;sup>2</sup> Present address: Department of Chemistry and Biochemistry, Southwestern University, Georgetown, Texas 78626, United States

<sup>&</sup>lt;sup>3</sup> Corresponding author. **Email**: gsengel@uchicago.edu

<sup>#</sup>Authors contributed equally to this work

#### Abstract

Quantum coherences, observed as time-dependent beats in ultrafast spectroscopic experiments, arise when light-matter interactions prepare systems in superpositions of states with differing energy and fixed phase across the ensemble. Such coherences have been observed in photosynthetic systems following ultrafast laser excitation, but what these coherences imply about the underlying energy transfer dynamics remains subject to debate. Recent work showed that redox conditions tune vibronic coupling in the Fenna-Matthews-Olson (FMO) pigment-protein complex in green sulfur bacteria, raising the question of whether redox conditions may also affect the longlived (>100 fs) quantum coherences observed in this complex. In this work, we perform ultrafast two-dimensional electronic spectroscopy measurements on the FMO complex under both oxidizing and reducing conditions. We observe that many excited state coherences are exclusively present in reducing conditions and are absent or attenuated in oxidizing conditions. Reducing conditions mimic the natural conditions of the complex more closely. Further, the presence of these coherences correlates with the vibronic coupling that produces faster, more efficient energy transfer through the complex under reducing conditions. The growth of coherences across the waiting time and the number of beating frequencies across hundreds of wavenumbers in the power spectra suggest that the beats are excited state coherences with mostly vibrational character whose phase relationship is maintained through the energy transfer process. Our results suggest that excitonic energy transfer proceeds through a coherent mechanism in this complex and that the coherences may provide a tool to disentangle coherent relaxation from energy transfer driven by stochastic environmental fluctuations.

## **Significance Statement**

Photosynthetic organisms evolved their light harvesting antenna complexes to optimize energy transfer. It was recently shown that the redox environment can tune the mixing of electronic and vibrational states to steer energy through different pathways of a pigment-protein complex. Quantum beating signals in spectra of pigment-protein complexes have been used to probe the excited state dynamics within the complexes, but the microscopic dynamics that generate these signals and their role in promoting energy transfer are not fully understood. Here, we show that the redox environment that tunes energy transfer similarly tunes the quantum beating signals in the same complex. We find that the beats report on excited state vibrations that maintain coherence through the vibronically enhanced energy transfer process.

#### Introduction

Photosynthesis relies on light harvesting pigment-protein complexes that absorb sunlight and transfer the energy to reaction centers (1). The growth, development, and productivity of a photosynthetic organism are bounded by how efficiently antenna complexes can funnel solar energy to reaction centers (2-4) and the robustness of these complexes to environmental damage. To optimize both light absorption and energy transfer, the protein both serves as a structural scaffold that holds the light-absorbing pigments at specific relative orientations and also a dissipative bath to facilitate relaxation (5). Both inter-pigment coupling and pigment-bath coupling contribute to the energy transfer dynamics of antenna complexes (6-8).

The microscopic motions that drive energy transfer can preserve the quantum coherence in a system. Quantum coherence is an ensemble phenomenon that results from sustained phase relationships between superpositions of states across space and time (9). It can be detected as time-domain beating signals in two-dimensional and pump-probe spectra. Dephasing and decoherence, which diminish the beating amplitude of the signal, depend critically on complex dynamical interactions between the system and the bath; therefore, quantum beats arising from coupling between excited states offer unique insight into system-bath interactions and the relevant energy transport dynamics of complex systems (10, 11). Long-lived quantum beats persisting for hundreds of femtoseconds to picoseconds have been observed in the FMO pigment-protein complex from green sulfur bacteria (8, 12-14). Although initially assigned to long-lived coherences between electronic states (8), later studies have hypothesized that these coherences arise from vibrational states on the ground state surface (15-17) or between vibronic states (18, 19), which could microscopically explain how the beats can persist for hundreds of femtoseconds. Vibronic states arise when excitonic states with different levels of vibrational excitation couple to form a new

basis of mixed electronic-vibrational states (20). Recent work using rephasing pathways to isolate excited state coherence signals has suggested that the purely electronic coherences in FMO dephase within 100 fs (19, 21). The longer lived coherences are likely a combination of ground state vibrational, and excited state vibrational, and vibronic coherences, though their functional role in photosynthetic light harvesting is not yet fully understood (22-25).

Changes in the redox environment of an antenna complex can additionally affect the observed photophysical and transport properties. In the FMO complex, the addition of an oxygenscavenging reducing agent, such as sodium dithionite, significantly enhances the fluorescence quantum yield (26). The addition of such a reducing agent mimics the physiological environment of green sulfur bacteria, which are anaerobic phototrophs that cannot survive in highly oxic environments (27). Recent work on the FMO complex identified a pair of cysteine residues (Figure 1A) that, upon oxidation of the side chain thiol to a thiyl radical, nonradiatively quench excitations via a charge transfer and recombination mechanism (28-30). Ultrafast spectroscopic experiments have shown that the excitonic transport dynamics through the FMO complex are faster under reducing conditions (31). In reducing conditions, the cysteine residues tune the resonant vibronic coupling between the excitons and pigment vibrations to enhance energy transfer, whereas in oxidizing conditions, the vibronic coupling is detuned to steer excitations toward the nonradiative quenching sites (32). These results showed that resonant vibrations play a definitive role in photosynthetic energy transport, as conceptualized originally by the Olaya-Castro group (33-35). In particular, quantized vibrations can promote non-sequential energy transport (33) – shown by the vibronically enhanced exciton 4-1 energy transfer in FMO in reducing conditions (32). Given the influence of redox on excitonic energy transport, it is likely that redox environment also affects excited state quantum beating signals observed in photosynthetic complexes.

In this work, we use two-dimensional electronic spectroscopy (2DES) to investigate how the long-lived quantum coherences observed in the FMO complex are affected by oxidizing and reducing conditions and the subsequent influence on energy transfer. We observe a positive relationship between enhanced quantum coherence signals and the vibronic coupling observed in reducing conditions (32). Using a spectral analysis method described previously (19), we find that under reducing conditions, the beating magnitudes of many long-lived coherences are increased relative to their magnitudes under oxidizing conditions and that many of the quantum beats appear as below-diagonal stimulated emission features in the 2D spectrum (i.e. features which result from downhill energy transfer in the excited state). The location of the long-lived coherences correlates with increased vibronic coupling and more efficient downhill energy transfer through the FMO complex (31, 32). The strength of beating increases with waiting time up to two picoseconds, which we ascribe to an excited state coherence transfer. The persistence of multiple beating frequencies below the diagonal and their growth with waiting time suggests that many of the coherences arise from excited state vibrational coherences that retain their phase relationship through the vibronically enhanced energy transfer process. The redox-dependent coherent behavior shown here suggests that sample preparation and handling between experiments may underlie much of the controversy surrounding the assignment of quantum coherences in biology.

#### **Results & Discussion**

Quantum Beats Correlate with Redox Conditions and Enhanced Energy Transport

Linear absorption spectra and 2D electronic spectra of the FMO complex at 77 K were collected under both oxidizing and reducing conditions using the same methods described previously (31, 32). The linear absorption spectra (**Figure 1B**) show that a change in the redox

condition shifts the peak positions of the absorption spectrum, previously shown to be due to the oxidation state of the cysteine residues C49 and C353 and likely other residues (30, 31). Two-dimensional electronic spectroscopy (2DES) can follow the time evolution of both population and coherence signals as they evolve through the waiting time, allowing us to investigate whether the coherent behavior of the FMO complex is redox-dependent. In 2DES, we illuminate the sample with four laser pulses to observe the molecular response as a function of the three time periods between pulses,  $R^{(3)}(\tau, T, t)$ . Using Fourier analysis and interpolation, we process the signal and cast the first and third domains into the frequency representation,  $Sig(\omega_{\tau}, T, \omega_{t})$ . Doing so allows us to correlate the excitation frequency of the system  $\omega_{\tau}$  with the detection frequency  $\omega_{t}$  at different waiting times T. Rephasing spectra for oxidized and reduced FMO are plotted in **Figure 1C-D** for T = 40 fs. These spectra show clear differences in the cross-peak amplitude between reducing and oxidizing conditions, indicating more efficient population transfer in reducing conditions that has been observed previously (31, 36). This enhanced efficiency is due to a resonant vibrational mode that couples excitons 4 and 1 (32).

Time-domain beats appear as signal oscillations during the waiting time T with a frequency proportional to the energy difference between the states (8, 11, 37, 38). To isolate the coherent beating signals, we remove the exponentially decaying contributions to the waiting time signals that correspond to population dynamics. We then Fourier transform the detrended traces to generate a waiting time frequency signal,  $Sig(\omega_{\tau}, \omega_{T}, \omega_{t})$ . To focus solely on the longer-lived coherences in the spectra, we only include data points after waiting time T = 240 fs in the Fourier transform. The oxidized and reduced data are normalized so that we can compare the relative magnitude of the spectral power between the two redox conditions (see **Supporting Information** for details and a beating analysis including earlier waiting times).

In rephasing pathways, the sign of the phase evolution during  $\tau$  is opposite to that of t because the state with higher energy switches from the bra to the ket in the t domain (19). Positive and negative wavenumbers in  $\omega_T$  report on coherences that oscillate in opposite directions in T (39, 40), corresponding to which state of the density matrix is higher in energy. This distinction enables differentiation between beating features occurring on the ground or excited state. For our 77 K experiments, ground state bleach contributions to the rephasing pathway can only oscillate at negative frequency in the beating maps because the first two interactions prepare a  $|g_0\rangle\langle g_v|$  coherence, where  $g_v$  denotes a higher vibrational state on the electronic ground state (11) (see Figure S16). The only ground state bleach pathways that give a positive frequency occur from an initially vibrationally excited ground state  $|g_v\rangle\langle g_v|$ ; however, these vibrations are suppressed because the necessary frequencies are several factors higher in energy than  $k_BT$  at the cryogenic temperatures measured here. Features that oscillate at positive frequencies therefore must be generated by stimulated emission or excited-state absorption pathways and thus report on electronic, vibrational, or vibronic coherences in the excited state (19).

Power spectra for all beating frequencies ωτ integrated over different regions of the 2D spectra are shown in **Figure 2**. In the negative waiting time frequencies of each region, we observe many beating frequencies that likely are ground state vibrational coherences. There are also many positive beating frequencies between 0 and +1000 cm<sup>-1</sup> that report on coherences in the excited state. Several of the observed frequencies are in good agreement with the fluorescence line narrowing spectra of FMO in the literature (41). Many coherences match the frequencies observed in two-dimensional spectra of isolated bacteriochlorophyll-*a* molecules reported by Fransted *et al*. (e.g. 730 cm<sup>-1</sup> and 550 cm<sup>-1</sup>) (42) and Ogilvie and coworkers (e.g. 201 cm<sup>-1</sup> and 348 cm<sup>-1</sup>) (24). In the diagonal spectra (**Figure 2E-F**), some frequencies are only present in reducing conditions (e.g.

the 335 cm<sup>-1</sup> and 378 cm<sup>-1</sup> pair in the exciton 4 diagonal region), but in general, many of the observed beats are similar in magnitude between redox conditions. In contrast, virtually all the positive beats in the below-diagonal beating spectra (Figure 2B-D) are higher in magnitude in reducing conditions than in oxidizing conditions. Because of the large number of observed frequencies, the beats likely report on energy gaps between states with mostly excited state vibrational character (6, 41, 43-45) rather than between purely electronic states. The belowdiagonal regions correspond to the downhill energy transfer that is enhanced in reducing conditions (Figure 1C-D) due to the tuned vibronic coupling shown in a previous study (32), further suggesting that the redox-dependent positive-frequency beats are related to the vibronic coupling present only in reducing conditions. Additionally, many negative frequencies are enhanced in reducing conditions in the below-diagonal cross peak regions. We assign these beats to ground state vibrational coherences that are enhanced by the vibronic states in reducing conditions, as has been shown and discussed extensively in the literature (18, 46-48). A more detailed analysis of this assignment can be found in the Supporting Information. Other integrated regions display similar overall trends and can be found in Figure S1.

We generate beating maps at specific waiting time frequencies to reveal quantifiable changes in the quantum beats throughout the 2D spectrum. The spectra for the +167 cm<sup>-1</sup>, +335 cm<sup>-1</sup>, and +550 cm<sup>-1</sup> coherent oscillations for both oxidizing and reducing conditions are shown in **Figure 3**. The magnitudes report on the relative strength of the beating signal at each point on the 2D spectrum. All beat maps for a given redox condition are normalized to the beating value of the summed frequency cube as described in the **Supporting Information**. At each frequency, there are clear differences between the two redox conditions. For the +167 cm<sup>-1</sup> beating maps (**Figure 3A, D**), both oxidized and reduced spectra show a feature of similar magnitude on the main

diagonal around 12,300 cm<sup>-1</sup>, corresponding to the exciton 2-4 energies. However, the lineshape of the diagonal feature of the beating map is different between redox conditions, and the diagonal peak width is larger in reducing conditions. Similar features are notably absent in the oxidized spectra for +335 cm<sup>-1</sup> and +550 cm<sup>-1</sup> (**Figure 3B, C**) but present in the corresponding reduced spectra (**Figure 3E, F**). Additionally, the reduced beating maps for the three frequencies show a clear below-diagonal peak centered at ~12,100 cm<sup>-1</sup> on the detection axis that is almost entirely absent in the oxidized measurements. This feature is in close proximity to the exciton 1 energy on the detection axis (43, 49). We observe the same structural pattern (i.e., below-diagonal features only present in reducing conditions) for several other positive beating frequencies, including 815 cm<sup>-1</sup> and 1082 cm<sup>-1</sup> (see **Figure S3-5, Figure S7**). Taken together, the region-specific power spectra in **Figure 2** and the beating maps in **Figure 3** show that many observed long-lived quantum beats correlate with vibronically enhanced energy transfer through the FMO complex (32).

#### Time Evolution of Excited State Vibrational Coherences

To better understand the time evolution of these excited state coherences, we apply a sliding window Fourier transform to the detrended waiting time traces. We apply a window in the waiting time domain with a 1000 fs width and center waiting time value, T' (50). **Figure 4B** shows a sliding window trace of the regionally averaged intensity of the below-diagonal beating feature in the reduced spectrum at +167 cm<sup>-1</sup>. The feature clearly grows in at larger T' values. This effect can also be seen in **Figure S11**, which shows a reduced beating spectrum for the +167 cm<sup>-1</sup> frequency at early (200 – 1200 fs) and later waiting times (1200 – 2200 fs). Both representations show that the beating intensities of the diagonal and below-diagonal features are greater at later waiting times. We show that the overall growth pattern of the +167 cm<sup>-1</sup> feature does not change

with different sliding window sizes in T (**Figure S9**) or the size of the averaged region in  $\omega_{\tau}$  and  $\omega_{t}$  (**Figure S10**). In **Figure S8** and **Figure S12**, we show the growth and decay patterns in other excited state coherences. Beating frequencies adjacent to +167 cm<sup>-1</sup> (125 cm<sup>-1</sup> and 203 cm<sup>-1</sup>) show qualitatively different trends, indicating that the sliding window Fourier transform does not affect all frequencies in the same manner. For a given beating frequency, there is a competition between growth due to coherence transfer and decay due to dephasing and decoherence (11). This interplay produces different behavior between beating frequencies as the bath couples differently to each mode. Sliding window time trace differences between frequencies indicate that the bath environment affects these two competing forces differently. Frequencies such as +550 and +1082 cm<sup>-1</sup> show similar growth to +167 cm<sup>-1</sup> (**Figure S12**), indicating that many of the below-diagonal beats present only in reducing conditions grow with waiting time.

The previous observation that vibronic coupling between excitons 4 and 1 enhances energy transfer efficiency under reducing conditions (32) correlates with the beating patterns we observe. However, given the number of frequencies we see in reducing conditions (**Figure 3**), it is unlikely that the coherences are between these particular vibronic states, as the beating frequencies cannot all match the 4-1 exciton energy gap. The observed beats span over ~1000 cm<sup>-1</sup> (**Figure 2**), so it is unlikely that the coherences arise from different pairs of vibronic states because the beats would otherwise span a smaller frequency window. Rather, the beating signals most likely arise from coherences with largely vibrational character. The consistency between the coherence frequencies of isolated bacteriochlorophyll-*a* and these beats supports this vibrational picture (24, 42). These coherences could be 'purely' vibrational or have small degrees of vibronic mixing with other excitonic surfaces. Either assignment would explain their long dephasing times and structural similarity in the beating spectra.

A proposed stimulated emission Feynman pathway that explains the beating signals is shown in Figure 4A. In this pathway, an excited state vibrational coherence starting on exciton 4 transfers to exciton 1 during the waiting time while maintaining the vibrational coherence. This latter coherence is observed as a below-diagonal beating signal. This is the most likely pathway for the beating signals because 1) the bra-ket energy difference is maintained over the energy transfer process, and 2) the position of the signals on the 2D spectrum is invariant to the energy of the excited vibration (see Supporting Information) (51, 52). Similar pathways have been prescribed in the bacterial reaction center in purple bacteria (53). Many excited state coherences of different excited state vibrational modes are accessed in the first two laser interactions in our experiment, which explains why we observe multiple beating frequencies in this region (Figure 3, Figure S7). The sliding window Fourier transform traces further support the downhill vibrational coherence transfer picture, as we see the growth of many modes with waiting time (Figure 4B, Figure S12). In this picture, the vibrational modes must be on a pigment or pigments where the two excitonic states overlap.

The process described here operates outside the typical assumptions for energy transfer because the vibrational coherence is not destroyed in the energy transfer process. The preserved coherence across multiple vibrational modes strongly suggests that the vibronically enhanced energy transfer must be a coherent process. In these data, the long-lived coherences present in reducing conditions are simply spectators to the enhanced energy transfer in reducing conditions. While the coherences themselves are largely vibrational in character, they are only observable because of the vibronic mixing that promotes energy transfer in the system. The vibrational coherences are thus sensitive probes of both enhanced energy transfer and the strong mixing of vibronic states in reducing conditions. Previous studies have shown that cooperative bath motion

around different pigments within a complex can maintain the lifetime of excited state coherences (54-57). These bath motions preserve the phase relationships across the ensemble due to the resonant vibronic coupling that promotes energy transfer in reducing conditions (58). Such preservation of phase necessitates coherence transfer alongside population transfer, implying significant non-secular terms in the relaxation superoperator (see Ref. (59)). A full quantum mechanical description of this process would require that all relevant vibrations be treated as part of the system. Within a semiclassical approximation considering only the electronic states explicitly, the bath must be treated parametrically such that the same bath motions affect the timevarying Hamiltonian operating on both sides of the density matrix. This semiclassical approximation shows explicitly how the same bath motions can drive simultaneous relaxation on both the bra- and the ket-states to preserve phase across the ensemble.

It is further possible that the resonant vibronic coupling induced in reducing conditions alters the excited state potential energy surfaces such that many excited state vibrational energies are markedly different from their ground state energies. This coupling would drastically change the Duschinsky rotation matrix and subsequently alter the absorption and emission vibrational profiles and, in turn, the excited state vibrational coherences (60). This effect may explain a number of coherences observed in this study that have not been observed in ground state spectroscopic experiments. The Duschinsky matrix has been calculated for isolated bacteriochlorophyll-a (44) and chlorophyll-a (60) molecules, and the subsequent effect on the excited state dynamics of light harvesting complexes has been discussed (60). Future high-resolution spectroscopic methods should investigate the effect that redox-induced vibronic coupling has on the excited state vibrational structure of the FMO complex and how Duschinsky rotation ties in with the preservation of coherence through the energy transfer process.

#### **Conclusions**

In this study, we observe excited state quantum beats in the FMO complex that are exclusively present in reducing conditions. The coherences are located in below-diagonal regions of the 2D spectrum that correspond to enhanced energy transfer due to vibronic coupling between excitons. The coherences exist at multiple beating frequencies, from ~100 cm<sup>-1</sup> to 1000 cm<sup>-1</sup>, indicating that the observed beats are likely excited state coherences with mostly vibrational character. Many of these coherences located on the below diagonal cross-peaks appear to increase in magnitude with waiting time, and we hypothesize that they result from a coherence transfer between excited state coherences on different excitonic surfaces (see Figure 4A, stimulated emission pathway). Interestingly, the location and growth of the coherences suggests that the vibronic coupling that enhances energy transfer in reducing conditions also preserves the coherence between a number of excited state vibrational modes. Coherence transfer has been previously observed and correlated with vibronic coupling in the reaction center of purple bacteria (53). Alternatively, it is possible that the coherence itself is actually growing or being spontaneously generated with time as suggested by Olaya-Castro and coworkers (33, 34) as well as Plenio, Huelga, and coworkers (61). Our results indicate that the redox condition of a pigmentprotein complex must be known when assigning an observed beat signal to a specific quantum coherence. Indeed, much of the debate in the literature regarding the nature of these long-lived coherences may result from differences in experimental sample preparation between research groups as both samples and reducing agents are air-sensitive. Our results also show that excited state coherences observed in these spectra can serve as reporters on the vibronically enhanced energy transfer through the complex.

### **Experimental Methods**

C. tepidum was grown, and FMO was isolated in CAPS (N-cyclohexyl-3-aminopropanesulfonic acid) buffer (pH 10.5) following well established literature procedures (30, 62-64). Measurements in this study were taken on a mixture of glycerol (50% by volume) and 20 mM CAPS-buffered (pH 10.5) FMO protein. Under oxidizing conditions, the samples were handled under ambient conditions without any further preparation; in the reducing case, sodium dithionite was added to the protein, buffer, and glycerol mixture to a concentration of 10 mM. The mixture was placed in a 200 μm quartz cuvette (Starna) that was prepared with a hydrophobic coating (SigmaCote, Sigma-Aldrich). The cuvette was loaded into a nitrogen-cooled cryostat (Oxford Instruments) and rapidly cooled to 77 K, forming a glass. The sample was held at 77 K for all measurements.

The 2D electronic spectra were acquired using the GRAPES single-shot spectrometer described in detail elsewhere (65-67). In these experiments, the output of an ultrafast regenerative amplifier (Legend Elite USP, Coherent) centered at 800 nm and running at a 5 kHz repetition rate was focused through a tube containing 15 psi of Ar gas. The broadened light was subsequently focused in air a second time to produce a spectrum that spans from 775 nm to 840 nm. This bandwidth was compressed to a < 20 fs laser pulse using an optical pulse shaper (MIIPS Box 640, Biophotonics Solutions) running a MIIPS algorithm (68). Beamsplitters generated four beams with parallel electric-field polarizations that were aligned to form a shifted boxcars geometry. Pulse 1 has a geometric tilt relative to pulses 2 and 3, meaning that different parts of the isotropic sample encode different coherence times, with 0.9 fs steps between different coherence times. Beams 1 and 2 were chopped together at 50 Hz and the signal was collected in the  $-k_1 + k_2 + k_3$  phasematched direction on the slit of an imaging spectrometer (Shamrock, Andor Technologies) and

recorded on a CMOS camera (Miro M310, Vision Research). Pulse 4 in the boxcar geometry was attenuated using a neutral-density filter and mixed with the signal on the camera to enable a phase-sensitive heterodyne detection of the signal field. The delay time between pulse 3 and the pulse 1-2 pair was swept continuously during acquisition using an optomechanical delay line (Aerotech, Inc.). Individual 2DES spectra were recorded at waiting times from -300 fs to +2240 fs with a 0.4 fs spacing. The rephasing pathways were isolated in post-processing by selecting the positive-valued coherence times.

The data were Fourier filtered in the waiting-time domain to remove scattered light, generating a final data set with 10 fs spacing between waiting times (67). The 2DES data were phased by fitting to separately acquired pump-probe data using a sum-of-squared-error regression. Each experiment was repeated to collect a total of 25 independent measurements that were subsequently averaged after phasing. Beating maps were generated by fitting the exponentially decaying dynamics of the phased, complex-valued data and subtracting the fit. The residuals of the full waiting time and the sliding window spectra were apodized, zero-padded out to 2001 total points, and then Fourier transformed.

## Acknowledgments

The authors thank Dr. Karen Watters and Dr. Monali Sawai for scientific editing. This work was supported by the Department of Defense as part of the Vannevar Bush Fellowship (N00014-16-1-2513), the Air Force Office of Scientific Research (FA9550-18-1-0099), and the DOE Office of Science (under award no. DE-SC0020131). NSF (under grant no. 1900359) supported efforts to analyze the data and model vibronic response. Additional support was provided by the Chicago MRSEC, which is funded by the NSF through grant DMR-1420709. M.A.A. acknowledges

support from an Arnold O. Beckman Postdoctoral Fellowship from the Arnold and Mabel Beckman Foundation and from a Yen Postdoctoral fellowship from the Institute for Biophysical Dynamics at The University of Chicago. J.S.H. was supported by the NSF-GRFP fellowship. S.H.S, R.E.W, and S.C.M were each supported individually by a National Defense Science and Engineering Graduate (NDSEG) Fellowship, 32 CFR 168a. R.E.B and R.G.S acknowledge funding from the Photosynthetic Antenna Research Center, an Energy Frontier Research Center funded by the U.S. Department of Energy, Office of Science, Office of Basic Energy Sciences, under Award DE-SC 0001035.

#### References

- 1. R. E. Blankenship, *Molecular mechanisms of photosynthesis* (Wiley/Blackwell, Chichester, West Sussex, ed. Second, 2014).
- 2. A. V. Ruban, Crops on the fast track for light. *Nature* **541**, 36 (2017).
- 3. R. K. Clayton, B. J. Clayton, B850 pigment-protein complex of Rhodopseudomonas sphaeroides: Extinction coefficients, circular dichroism, and the reversible binding of bacteriochlorophyll. *Proc. Natl. Acad. Sci. USA* **78**, 5583-5587 (1981).
- 4. Z. Liu *et al.*, Crystal structure of spinach major light-harvesting complex at 2.72 Å resolution. *Nature* **428**, 287-292 (2004).
- 5. R. Fenna, B. Matthews, Chlorophyll arrangement in a bacteriochlorophyll protein from Chlorobium limicola. *Nature* **258**, 573-577 (1975).
- 6. T. Brixner *et al.*, Two-dimensional spectroscopy of electronic couplings in photosynthesis. *Nature* **434**, 625-628 (2005).
- 7. J. Dostál, J. Pšenčík, D. Zigmantas, In situ mapping of the energy flow through the entire photosynthetic apparatus. *Nat. Chem.* **8**, 705-710 (2016).
- 8. G. S. Engel *et al.*, Evidence for wavelike energy transfer through quantum coherence in photosynthetic systems. *Nature* **446**, 782-786 (2007).
- 9. G. D. Scholes *et al.*, Using coherence to enhance function in chemical and biophysical systems. *Nature* **543**, 647 (2017).
- 10. S. Lloyd *et al.*, No energy transport without discord. arXiv:1510.05035 (2015).
- 11. S. Mukamel, *Principles of Nonlinear Optical Spectroscopy* (Oxford University Press, New York, 1995).
- 12. S. Savikhin, D. R. Buck, W. S. Struve, Oscillating anisotropies in a bacteriochlorophyll protein: Evidence for quantum beating between exciton levels. *Chem. Phys.* **223**, 303-312 (1997).
- 13. G. Panitchayangkoon *et al.*, Long-lived quantum coherence in photosynthetic complexes at physiological temperature. *Proc. Natl. Acad. Sci. USA* **107**, 12766-12770 (2010).
- 14. E. Collini *et al.*, Coherently wired light-harvesting in photosynthetic marine algae at ambient temperature. *Nature* **463**, 644-647 (2010).
- 15. V. Tiwari, W. K. Peters, D. M. Jonas, Electronic resonance with anticorrelated pigment vibrations drives photosynthetic energy transfer outside the adiabatic framework. *Proc. Natl. Acad. Sci. USA* **110**, 1203-1208 (2013).
- 16. M. Maiuri, E. E. Ostroumov, R. G. Saer, R. E. Blankenship, G. D. Scholes, Coherent wavepackets in the Fenna–Matthews–Olson complex are robust to excitonic-structure perturbations caused by mutagenesis. *Nat. Chem.* **10**, 177 (2018).
- 17. R. Tempelaar, T. L. Jansen, J. Knoester, Vibrational beatings conceal evidence of electronic coherence in the FMO light-harvesting complex. *J. Phys. Chem. B* **118**, 12865-12872 (2014).
- 18. N. Christensson, H. F. Kauffmann, T. Pullerits, T. Mančal, Origin of Long-Lived Coherences in Light-Harvesting Complexes. *Journal of Physical Chemistry B* **116**, 7449-7454 (2012).
- 19. E. Thyrhaug *et al.*, Identification and characterization of diverse coherences in the Fenna–Matthews–Olson complex. *Nature Chemistry* **10**, 780-786 (2018).
- 20. L. Wang, M. A. Allodi, G. S. Engel, Quantum coherences reveal excited-state dynamics in biophysical systems. *Nature Reviews Chemistry* **3**, 477-490 (2019).

- 21. S. Irgen-Gioro, K. Gururangan, R. G. Saer, R. E. Blankenship, E. Harel, Electronic coherence lifetimes of the Fenna-Matthews-Olson complex and light harvesting complex II. *Chem Sci* **10**, 10503-10509 (2019).
- 22. S. Irgen-Gioro, A. P. Spencer, W. O. Hutson, E. Harel, Coherences of Bacteriochlorophyll a Uncovered Using 3D-Electronic Spectroscopy. *J Phys Chem Lett* **9**, 6077-6081 (2018).
- 23. S. Irgen-Gioro, K. Gururangan, A. P. Spencer, E. Harel, Non-Uniform Excited State Electronic-Vibrational Coupling of Pigment-Protein Complexes. *J Phys Chem Lett* 10.1021/acs.jpclett.0c02454, 10388-10395 (2020).
- 24. V. R. Policht, A. Niedringhaus, J. P. Ogilvie, Characterization of Vibrational Coherence in Monomeric Bacteriochlorophyll a by Two-Dimensional Electronic Spectroscopy. *J Phys Chem Lett* **9**, 6631-6637 (2018).
- 25. E. A. Arsenault, Y. Yoneda, M. Iwai, K. K. Niyogi, G. R. Fleming, Vibronic mixing enables ultrafast energy flow in light-harvesting complex II. *Nat Commun* 11, 1460 (2020).
- 26. W. Zhou, R. LoBrutto, S. Lin, R. E. Blankenship, Redox effects on the bacteriochlorophyll α-containing Fenna-Matthews-Olson protein from Chlorobium tepidum. *Photosynth. Res.* 41, 89-96 (1994).
- 27. T. M. Wahlund, C. R. Woese, R. W. Castenholz, M. T. Madigan, A thermophilic green sulfur bacterium from New Zealand hot springs, Chlorobium tepidum sp. nov. *Arch. Microbiol.* **156**, 81-90 (1991).
- 28. R. Saer *et al.*, Perturbation of bacteriochlorophyll molecules in Fenna–Matthews–Olson protein complexes through mutagenesis of cysteine residues. *Biochim. Biophys. Acta Bioenergetics* **1857**, 1455-1463 (2016).
- 29. J. Wen, H. Zhang, M. L. Gross, R. E. Blankenship, Membrane orientation of the FMO antenna protein from Chlorobaculum tepidum as determined by mass spectrometry-based footprinting. *Proc. Natl. Acad. Sci. USA* **106**, 6134-6139 (2009).
- 30. G. S. Orf *et al.*, Evidence for a cysteine-mediated mechanism of excitation energy regulation in a photosynthetic antenna complex. *Proceedings of the National Academy of Sciences* **113**, E4486-E4493 (2016).
- 31. M. A. Allodi *et al.*, Redox Conditions Affect Ultrafast Exciton Transport in Photosynthetic Pigment–Protein Complexes. *The Journal of Physical Chemistry Letters* **9**, 89-95 (2018).
- 32. J. S. Higgins *et al.*, Photosynthesis tunes quantum mechanical mixing of electronic and vibrational states to steer exciton energy transfer. *Proceedings of the National Academy of Sciences* (2021).
- 33. A. Kolli, E. J. O'Reilly, G. D. Scholes, A. Olaya-Castro, The fundamental role of quantized vibrations in coherent light harvesting by cryptophyte algae. *J Chem Phys* **137**, 174109 (2012).
- 34. E. J. O'Reilly, A. Olaya-Castro, Non-classicality of the molecular vibrations assisting exciton energy transfer at room temperature. *Nature Communications* **5**, 3012 (2014).
- 35. R. Stones, A. Olaya-Castro, Vibronic Coupling as a Design Principle to Optimize Photosynthetic Energy Transfer. *Chem* 1, 822-824 (2016).
- 36. P. Hamm, M. T. Zanni, *Concepts and methods of 2D Infrared Spectroscopy* (Cambridge UP, 2011).
- 37. R. S. Knox, Electronic excitation transfer in the photosynthetic unit: Reflections on work of William Arnold. *Photosynthesis Research* **48**, 35-39 (1996).

- 38. J. A. Leegwater, Coherent versus Incoherent Energy Transfer and Trapping in Photosynthetic Antenna Complexes. *Journal of Physical Chemistry* **100**, 14403-14409 (1996).
- 39. V. Butkus, L. Valkunas, D. Abramavicius, Vibronic phenomena and exciton-vibrational interference in two-dimensional spectra of molecular aggregates. *Journal of Chemical Physics* **140**, 034306 (2014).
- 40. V. Butkus *et al.*, Discrimination of Diverse Coherences Allows Identification of Electronic Transitions of a Molecular Nanoring. *Journal of Physical Chemistry Letters* **8**, 2344-2349 (2017).
- 41. M. Rätsep, A. Freiberg, Electron–phonon and vibronic couplings in the FMO bacteriochlorophyll a antenna complex studied by difference fluorescence line narrowing. *J. Lumin.* **127**, 251-259 (2007).
- 42. K. A. Fransted, J. R. Caram, D. Hayes, G. S. Engel, Two-dimensional electronic spectroscopy of bacteriochlorophyll a in solution: Elucidating the coherence dynamics of the Fenna-Matthews-Olson complex using its chromophore as a control. *The Journal of Chemical Physics* **137**, 125101 (2012).
- 43. M. Cho, H. M. Vaswani, T. Brixner, J. Stenger, G. R. Fleming, Exciton Analysis in 2D Electronic Spectroscopy. *J. Phys. Chem. B* **109**, 10542-10556 (2005).
- 44. M. Rätsep, Z.-L. Cai, J. R. Reimers, A. Freiberg, Demonstration and interpretation of significant asymmetry in the low-resolution and high-resolution Qy fluorescence and absorption spectra of bacteriochlorophyll a. *Journal of Chemical Physics* **134**, 024506 (2011).
- 45. M. Ceccarelli, M. Lutz, M. Marchi, A Density Functional Normal Mode Calculation of a Bacteriochlorophyll a Derivative. *Journal of the American Chemical Society* **122**, 3532-3533 (2000).
- 46. V. Tiwari, W. K. Peters, D. M. Jonas, Electronic resonance with anticorrelated pigment vibrations drives photosynthetic energy transfer outside the adiabatic framework. *Proceedings of the National Academy of Sciences* **110**, 1203 (2013).
- 47. M. B. Plenio, J. Almeida, S. F. Huelga, Origin of long-lived oscillations in 2D-spectra of a quantum vibronic model: electronic versus vibrational coherence. *J Chem Phys* **139**, 235102 (2013).
- 48. A. Chenu, N. Christensson, H. F. Kauffmann, T. Mancal, Enhancement of vibronic and ground-state vibrational coherences in 2D spectra of photosynthetic complexes. *Sci Rep* 3, 2029 (2013).
- 49. D. Hayes, Gregory S. Engel, Extracting the Excitonic Hamiltonian of the Fenna-Matthews-Olson Complex Using Three-Dimensional Third-Order Electronic Spectroscopy. *Biophysical Journal* **100**, 2043-2052 (2011).
- 50. S. M. Hart, J. L. Banal, M. Bathe, G. S. Schlau-Cohen, Identification of Nonradiative Decay Pathways in Cy3. *The Journal of Physical Chemistry Letters* **11**, 5000-5007 (2020).
- 51. L. Wang *et al.*, Controlling quantum-beating signals in 2D electronic spectra by packing synthetic heterodimers on single-walled carbon nanotubes. *Nature Chemistry* **9**, 219-225 (2017).
- 52. D. B. Turner *et al.*, Quantitative investigations of quantum coherence for a light-harvesting protein at conditions simulating photosynthesis. *Physical Chemistry Chemical Physics* **14**, 4857-4874 (2012).

- 53. V. N. Policht, A.; Willow, R.; Laible, P.; Bocian, D.; Kirmaier, C; Holten, D.; Mančal, T.; Ogilvie, J., Hidden Vibronic and Excitonic Structure and Vibronic Coherence Transfer in the Bacterial Reaction Center. *arXiv* (2021).
- 54. A. Olaya-Castro, C. F. Lee, F. F. Olsen, N. F. Johnson, Efficiency of energy transfer in a light-harvesting system under quantum coherence. *Physical Review B* **78** (2008).
- 55. P. Rebentrost, M. Mohseni, A. Aspuru-Guzik, Role of Quantum Coherence and Environmental Fluctuations in Chromophoric Energy Transport. *The Journal of Physical Chemistry B* **113**, 9942-9947 (2009).
- 56. F. Fassioli, A. Nazir, A. Olaya-Castro, Quantum State Tuning of Energy Transfer in a Correlated Environment. *The Journal of Physical Chemistry Letters* **1**, 2139-2143 (2010).
- 57. A. Olaya-Castro, G. D. Scholes, Energy transfer from Förster–Dexter theory to quantum coherent light-harvesting. *International Reviews in Physical Chemistry* **30**, 49-77 (2011).
- 58. M. Yang, G. Fleming, Influence of phonons on exciton transfer dynamics: comparison of the Redfield, Förster, and modified Redfield equations. *Chemical Physics* **275**, 355-372 (2002).
- 59. P. A. Eckert, K. J. Kubarych, Vibrational coherence transfer illuminates dark modes in models of the FeFe hydrogenase active site. *The Journal of Chemical Physics* **151**, 054307 (2019).
- 60. J. R. Reimers, M. Rätsep, A. Freiberg, Asymmetry in the Qy Fluorescence and Absorption Spectra of Chlorophyll a Pertaining to Exciton Dynamics. *Frontiers in Chemistry* **8** (2020).
- 61. A. W. Chin *et al.*, The role of non-equilibrium vibrational structures in electronic coherence and recoherence in pigment–protein complexes. *Nature Physics* **9**, 113-118 (2013).
- 62. Y.-F. Li, W. Zhou, R. E. Blankenship, J. P. Allen, Crystal structure of the bacteriochlorophyll a protein from Chlorobium tepidum. *Journal of molecular biology* **271**, 456-471 (1997).
- 63. P. D. Gerola, J. M. Olson, A new bacteriochlorophyll a-protein complex associated with chlorosomes of green sulfur bacteria. *Biochim. Biophys. Acta Bioenergetics* **848**, 69-76 (1986).
- 64. J. Wen, H. Zhang, M. L. Gross, R. E. Blankenship, Native electrospray mass spectrometry reveals the nature and stoichiometry of pigments in the FMO photosynthetic antenna protein. *Biochemistry* **50**, 3502-3511 (2011).
- 65. E. Harel, A. F. Fidler, G. S. Engel, Real-time mapping of electronic structure with single-shot two-dimensional electronic spectroscopy. *Proc. Natl. Acad. Sci. USA* **107**, 16444-16447 (2010).
- 66. E. Harel, A. F. Fidler, G. S. Engel, Single-Shot Gradient-Assisted Photon Echo Electronic Spectroscopy. *J. Phys. Chem. A* **115**, 3787-3796 (2011).
- 67. P. D. Dahlberg, A. F. Fidler, J. R. Caram, P. D. Long, G. S. Engel, Energy Transfer Observed in Live Cells Using Two-Dimensional Electronic Spectroscopy. *Journal of Physical Chemistry Letters* **4**, 3636-3640 (2013).
- 68. V. V. Lozovoy, I. Pastirk, M. Dantus, Multiphoton intrapulse interference. IV. Ultrashort laser pulse spectral phase characterization and compensation. *Opt. Lett.* **29**, 775-777 (2004).

## **Figures**

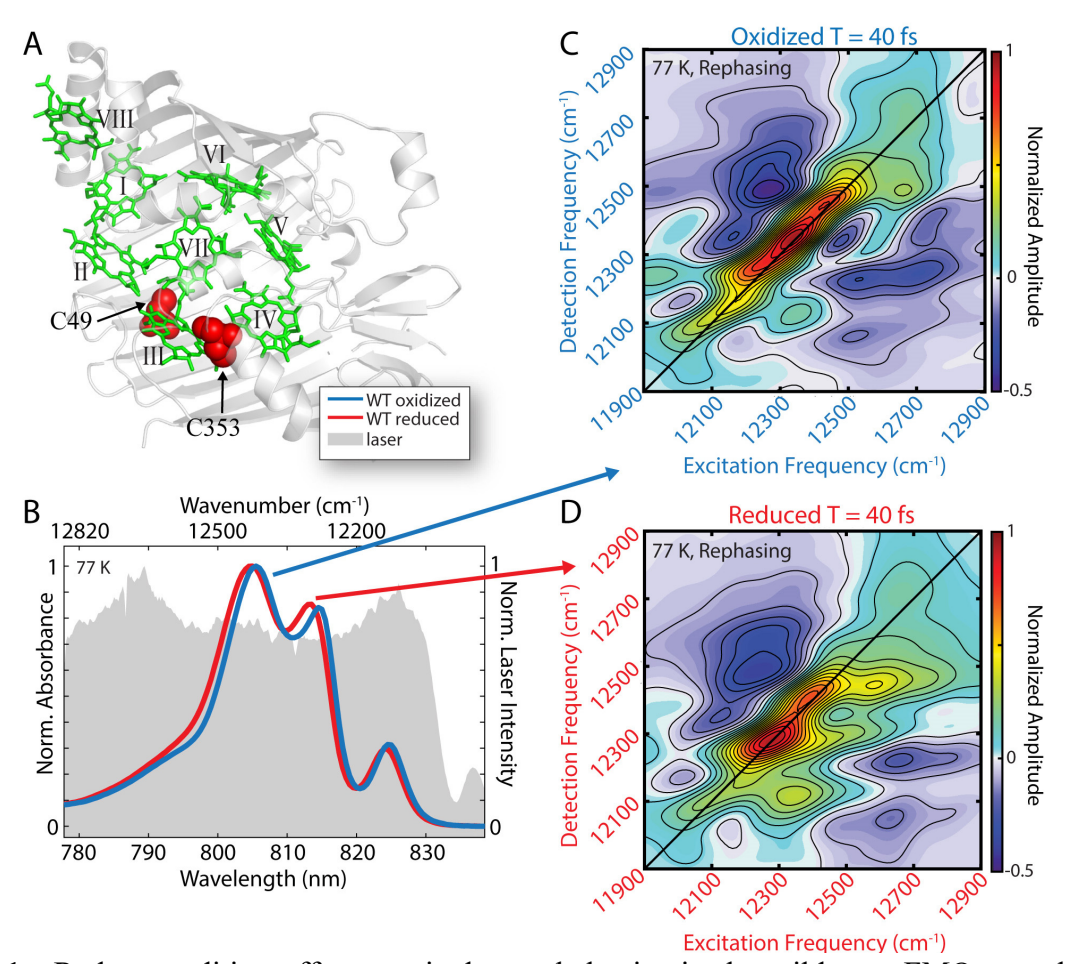


**Figure 1.** Redox condition affects excited state behavior in the wild-type FMO complex. **A**) Structure of the FMO complex and the eight bacteriochlorophyll-*a* sites held by the protein scaffold (PDB: 3ENI) (29). Shown in red are the two cysteine residues, C49 and C353, that are known to steer and quench excitations in oxidizing conditions and tune vibronic coupling for enhanced energy transfer in reducing conditions (30, 32). **B**) Linear absorption spectra of the wild-type oxidized (blue) and wild-type reduced (red) FMO complex at 77 K. Shown in gray is the laser spectrum used. **C**, **D**) Rephasing 2D electronic spectra under oxidizing and reducing conditions at waiting time T = 40 fs. Differences in the lower-diagonal cross peaks between experiments indicate faster, more efficient energy transfer when the complex is reduced.

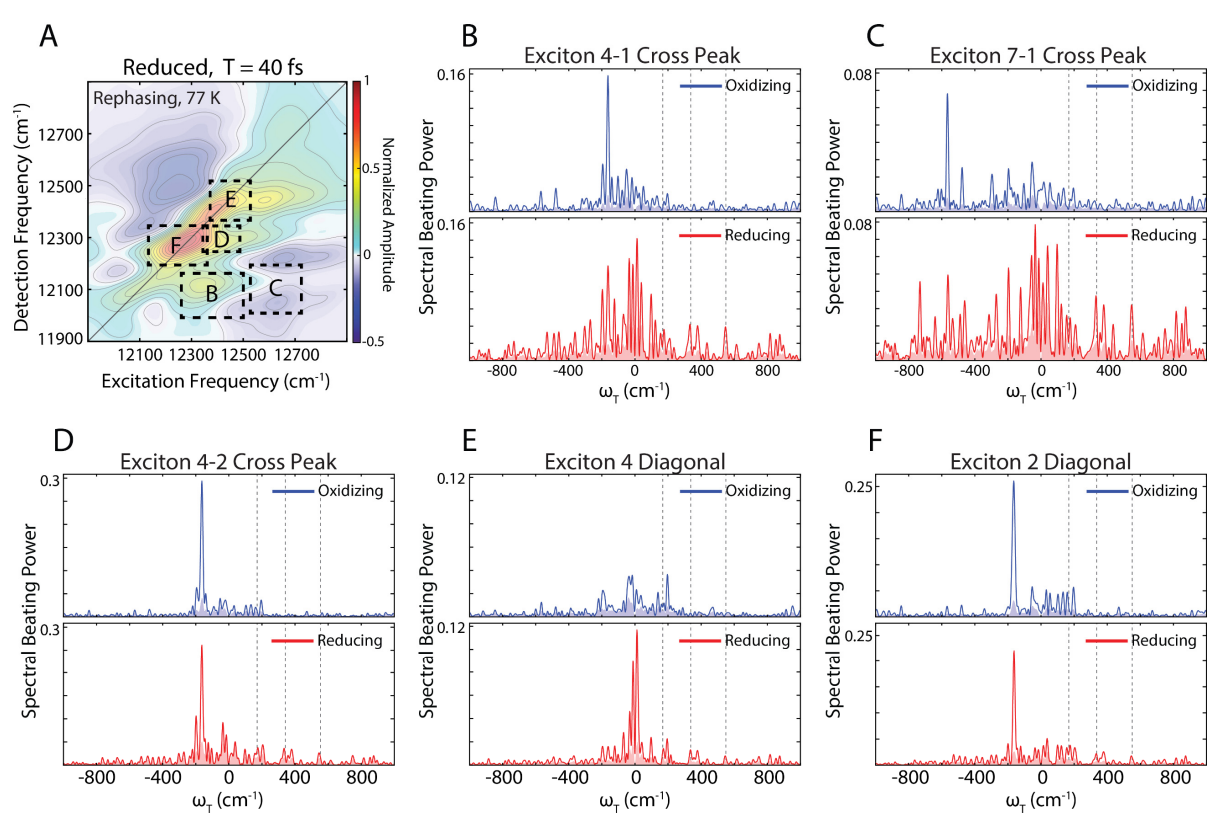


**Figure 2.** Rephasing power spectra for oscillations in T integrated over regions of the 2D spectrum. **A**) Reduced FMO 2D spectrum at T = 40 fs showing integrated regions. Regional power spectra for **B-D**) below-diagonal regions and **E-F**) diagonal regions. Oxidizing and reducing data are plotted in blue and red, respectively. The shaded regions represent the standard error over the mean. The dashed vertical lines mark positive beating frequencies at 167 cm<sup>-1</sup>, 335 cm<sup>-1</sup>, and 550 cm<sup>-1</sup>, shown as beating maps in the next figure. In general, the magnitude of the beating signals is larger in the reduced data below the diagonal, particularly at positive frequencies, which result from coherences on the excited state. Diagonal power spectra show similar beating magnitudes between redox conditions. All time traces were Fourier transformed after T = 240 fs to focus on the long-lived coherent dynamics. Other integrated regions can be found in **Figure S1**.

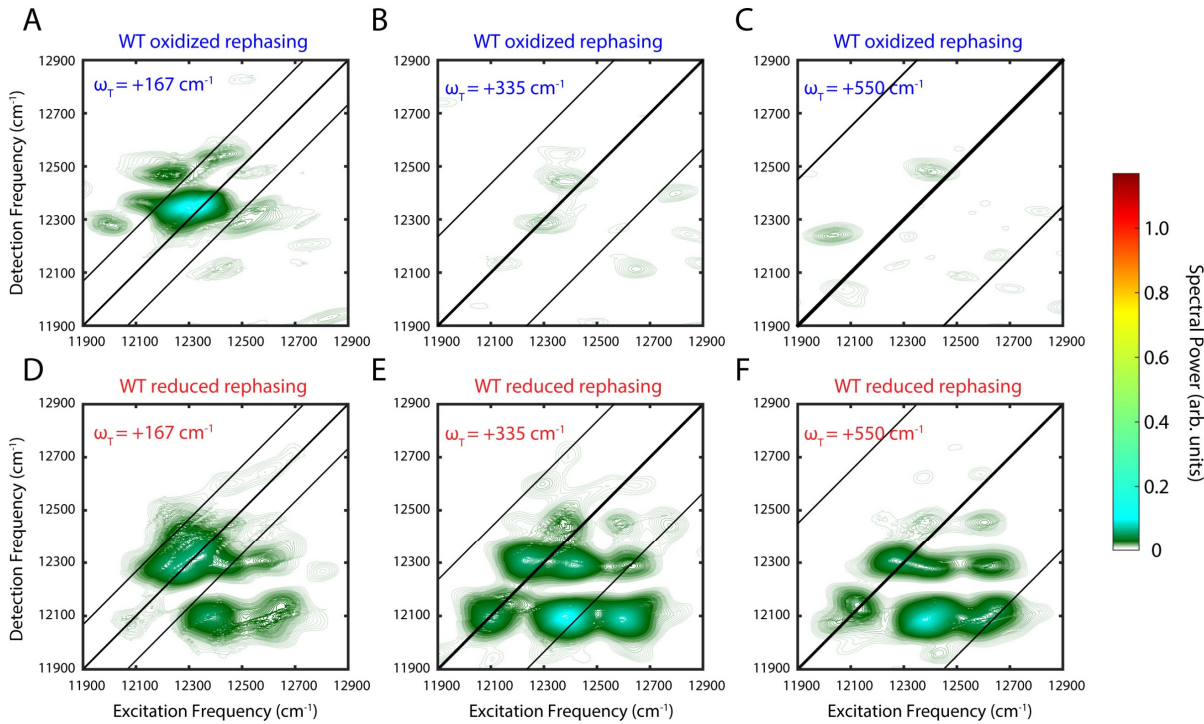


**Figure 3.** Beating amplitude maps at  $(\mathbf{A}, \mathbf{D})$  +167 cm<sup>-1</sup>,  $(\mathbf{B}, \mathbf{E})$  +335 cm<sup>-1</sup>, and  $(\mathbf{C}, \mathbf{F})$  +550 cm<sup>-1</sup> for rephasing FMO spectra under oxidizing and reducing conditions. The magnitude represents the relative beating strength for the  $\omega_T$  frequency at each point on the 2D spectrum. A below-diagonal feature at the positive frequency only appears in reducing conditions. This region corresponds to downhill energy transfer in the complex, which is enhanced in reducing conditions (31, 32).

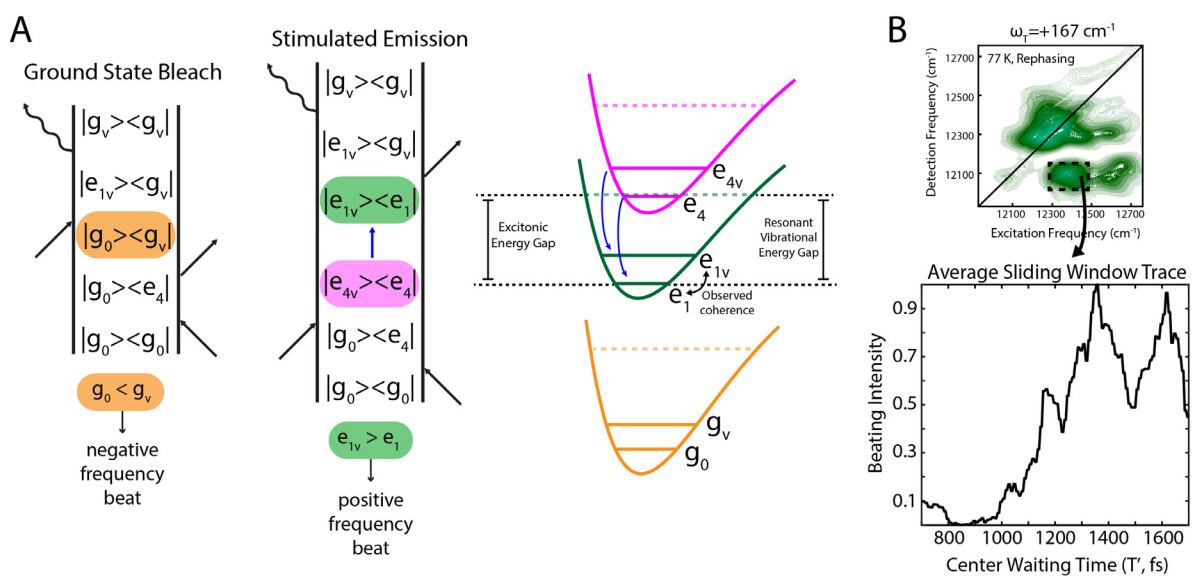


**Figure 4.** Proposed Feynman pathway explaining below-diagonal coherences observed at positive frequencies in the rephasing spectra. **A)** Ground state bleach pathways cannot contribute to the positive frequency because the energy of  $g_v$ , where the subscript v denotes an excited vibrational quantum, is greater than  $g_0$ , producing a negative frequency in T. The stimulated emission pathway contains a coherence transfer during T between excited state vibrational coherences on excitons 4 and 1. The observed beats below the diagonal are the vibrational coherences on exciton 1. Because  $e_{1v} > e_1$ , the waiting time frequency is positive. The enhanced energy transfer promoted by vibronic coupling in reducing conditions preserves the vibrational coherence (32). **B)** Sliding window Fourier transform of the below-diagonal feature at +167 cm<sup>-1</sup> using a 1000 fs window in T. The sliding trace shows that the coherence grows in with T, providing evidence for the coherence transfer pathway